

Tribological Properties of Polyimide Coatings Filled with PTFE and Surface-Modified Nano-Si₃N₄

Fenghua Su,^{1,2} Shaohua Zhang¹

¹School of Mechanical and Automotive Engineering, South China University of Technology, Guangzhou 510640, People's Republic of China

²State Key Laboratory of Solid Lubrication, Lanzhou Institute of Chemical Physics, Chinese Academy of Sciences, Lanzhou 730000, People's Republic of China

Correspondence to: F. Su (E-mail: fhsu@scut.edu.cn)

ABSTRACT: Polyimide (PI) coatings filled with PTFE and nano-Si₃N₄ were prepared by a spraying technique and successive curing. Nano-Si₃N₄ particles were modified by grafting 3-aminopropyltriethoxysilane to improve their dispersion in the as-prepared coatings. Friction and wear performances and wear mechanisms of the coatings were evaluated. The results show that the incorporations of PTFE and modified nano-Si₃N₄ particles greatly improve the friction reduction and wear resistance of PI coating. The friction and wear performance of the composite coating is significantly affected by the filler mass fraction and sliding conditions. PI coating incorporated with 20 wt % PTFE and 5 wt % modified nano-Si₃N₄ displays the best tribological properties. Its wear rate is more than one order of magnitude lower and its friction coefficient is over two times smaller than that of the unfilled PI coating. Differences in the friction and wear behaviors of the hybrid coatings as a function of filler or sliding condition are attributed to the filler dispersion, the characteristic of transfer film formed on the counterpart ball and the wear mechanism of the coating under different sliding conditions. © 2014 Wiley Periodicals, Inc. *J. Appl. Polym. Sci.* **2014**, *131*, 40410.

KEYWORDS: coatings; composites; friction; wear and lubrication; nanoparticles; nanowires and nanocrystals; polyimides

Received 4 November 2013; accepted 9 January 2014

DOI: 10.1002/app.40410

INTRODUCTION

Polymer composite coatings are particularly significant in reducing friction and wear as well as extending service life of facilities that are involved in surface contact and relative motion due to their low shear strength and good toughness. They are usefully applied in automotive components and other engineering applications, such as conveyor aids, chute liners, mining, agriculture, etc. Many polymer resins, including polyurethanes,¹ phenolics,² epoxies,³ acrylates,⁴ and poly (furfuryl alcohols),⁵ have been used as the matrices to prepare the polymer composite coatings.

The high performance, including high service temperature, good chemical resistance and outstanding mechanical strength, are always necessary for the polymer coatings in their engineering applications. Polyimide (PI) is considered to be a high performance polymer material due to their excellent mechanical strength, acceptable wear resistance under certain conditions, good thermal stability, high-stability under vacuum, good anti-radiation, and good solvent resistance. Its aromatic ring structures restrict the chain rotational freedom and moisture is an additional limitation for orientation.⁶ The preparation of PI based composites and

their friction and wear performances have been done by many researchers.^{7–12} Cai et al.⁷ investigated the mechanical and tribological properties of PI/CNTs composite produced by a hot compression molding. Zhang et al.⁸ used a hot press molding technique to prepare PI composite that was filled with carbon fiber, SiO₂ particles and graphite. The friction and wear properties of the as-prepared PI hybrid composite sliding against GCr15 steel were studied by a ring-on-block wear tester under different conditions. When compared to the bulk of literatures concerning PI based composites, literatures concerning the tribological properties of PI coatings are limited.^{12–14} Pozdnyakov et al.¹² studied the sliding wear of PI-C₆₀ composite coatings using a flat-on-ring friction geometry. They found that the friction coefficient (around 0.25) of PI and PI-C₆₀ composite coatings only slightly determined by the preparation conditions of the coatings and the presence of C₆₀. But the introduction of C₆₀ greatly improved the wear resistance of the coatings with a specific wear rate below $2 \times 10^{-7} \text{ mm}^3 (\text{Nm})^{-1}$ when the coating treatment took place at high temperature. Kim et al.¹³ evaluated the friction and wear performance of PI nanocomposite coatings reinforced with PMMA-grafted-MWCNTs. They confirmed that the nanocomposite

coating reinforced with 3 wt % MWCNT was the most stable and had the lowest coefficient of friction due to the formation of a thin, uniform friction film on the wear track during sliding.

To improve the friction characteristics and contribute to the control of wear, solid lubricants such as PTFE, MoS₂ and graphite flakes are frequently incorporated in the polymer matrix.^{2,15–19} Recently, nanoparticles are attracting increasing attention to improve the mechanical strength and wear resistance of polymer composites.^{2–4,20–23} Song et al.² confirmed that the solid lubricants of PTFE and PFW significantly improved the friction reduction and wear resistance of phenolic coatings. Kang et al.³ showed that the epoxy coating doped with a proper amount of nano-SiO₂ had lower friction coefficient and better wear resistance than the unfilled one. Zhang et al.⁴ confirmed that the incorporations of 40 wt % nano-SiO₂ particles reduced the friction coefficient of 20% and improved the wear resistance over 70 times for the acrylate coating at the same fretting test condition. Shi et al.⁸ verified that the wear resistance of the PTFE/PI composites was greatly improved by filling nanometer TiO₂ particles.

Although nano-composite often performs better than micro-composite, the specific surface area of nanoparticles is larger due to their small size effect, resulting in the probability of agglomeration of nanoparticles in matrix. The addition of such agglomerate nanoparticles into polymer composite is not sufficient for reaching a homogeneous dispersion state and thus degrades the improving level of the composite properties. The unique nano-effect of nanoparticle filler cannot be fully brought into play. In fact, surface modification was always used to modify nanoparticles and then enhance their reinforcing effect in composite.^{20,24–26} In this work, nano-Si₃N₄ particles were grafted with 3-aminopropyltriethoxysilane to improve their dispersions in the PI coating. The PI coatings filled with PTFE and nano-Si₃N₄ were produced by a spraying technique and successive curing. Effect of the treatment of nano-Si₃N₄ and sliding conditions on friction and wear performances of the resulting composite coatings were comparatively investigated using a ball-on-disk tribometer. Finally, the worn surfaces of the coatings and the transfer films formed on the counterpart balls were analyzed to illustrate the wear mechanisms of the coatings under different sliding conditions.

EXPERIMENTAL

Materials

The adhesive resin of polyamic acid (PAA-COOH, YJ-16) with ash content of 25 wt % were commercially supplied from Shanghai Synthetic Resin Institute (Shanghai, China). The PAA-COOH will be changed to be polyimide (PI) resin after thermocuring. Nano-Si₃N₄ with a diameter around 25 nm was provided by Hefei Kaier Nanometer Energy and Technology, China. Ethanol, which is analysis grade reagent, was purchased from Tianjin No. 1 Chemical Reagent Plant, China. PTFE particles with a diameter of 2.0–5.0 μm were provided by Beijing Sino-Rich, China. The 3-aminopropyltriethoxysilane (KH550) was purchased from Nanjing Xiangqian Chemical, China.

Modification of Nano-Si₃N₄ and FTIR Analysis

Nearly 60.0 ml ethanol, 10.0 ml KH550, and 5.0 g nano-Si₃N₄ were added into a flask and stirred with assistance of ultrasonic

for 10 min. Then, the solution was heated and maintained at 70°C for 5 h until the reaction was completed with assistance of mechanical stirring. After that, the KH550 modified nano-Si₃N₄ was filtered and cleaned with ethanol and dried in vacuum at 80°C for 12 h. Trace amount of the pure and modified nano-Si₃N₄ was added to prepare KBr pellets, which was then employed for Fourier transform infrared (FTIR) analysis. FTIR spectra were recorded on a Bruker Vector 33 FT-IR Spectrometer in the range of 400–4000 cm⁻¹. The untreated and modified nano-Si₃N₄ was dubbed as Si₃N₄-I and Si₃N₄-II, respectively, in subsequent sections.

Preparation and Morphology of the Coatings

Forty five steel plates with a dimension of Ø 30.0 × 2.0 mm² were used as substrate for the coatings. Surface of the steel plate was mechanically polished to a 0.20–0.30 μm surface finish with grade waterproof abrasive paper, and cleaned ultrasonically with acetone to remove contamination. The manufacture process of the composite coating of PI/PTFE was follows: PTFE powders with a mass fraction of 20.0 wt % was added in PAA-COOH adhesive resin and then carefully mixed by mechanical stirring and ultrasonication to obtain uniform slurry containing PAA-COOH and PTFE. Then, the uniform slurry were sprayed on steel substrate with 0.2–0.5 MPa air using a W-101 Iwata air spray gun and cured at 60°C for 4.0 h, 100°C for 1.0 h, 150°C for 2.0 h, 200°C for 1.5 h, and 280°C for 2.0 h to obtain PI/20wt%PTFE composite coating (dubbed as Coating-II). As a reference, pure PI coating (dubbed as Coating-I) was prepared in the same manner except no addition of PTFE.

The manufacture process of the composite coating of PI/PTFE/nano-Si₃N₄ was as follows: pure or modified nano-Si₃N₄ particles with desired proportion were first added in PAA-COOH adhesive resin and the mixture was carefully mixed by mechanical stirring and ultrasonication to obtain an even dispersion of nano-Si₃N₄ in the adhesive resin. After that, PTFE powders with a mass fraction of 20 wt % was added in the mixture and then was treated again with mechanical stirring and ultrasonication to obtain a uniform slurry containing PAA-COOH, nano-Si₃N₄ and PTFE. Then the uniform slurry was sprayed on steel substrate and cured with the same manner of producing Coating-II to obtain the composite coatings of PI/PTFE/nano-Si₃N₄. In this work, 5 wt % pure and modified nano-Si₃N₄ filled PI/20 wt %PTFE composite coatings are dubbed as Coating-III and Coating-IV, respectively. The mass fraction of PTFE and nano-Si₃N₄ means their relative content to the ash content of the adhesive resin. The surface and the cross-section of the resulting coatings were characterized using a FEI Quanta 200 scanning electron microscope (SEM). Element distributions in the coating were measured by an Energy Dispersed X-ray Analysis attached with a Quanta 200 SEM.

Characterization of the Friction and Wear Performances

The friction and wear behaviors of the composite coatings sliding against 5.0-mm diameter GCr15 steel ball were tested on a ball-on-disk MS-T3000 tribometer (Lanzhou Huahui Instrument Technology, China). Figure 1 shows the schematic diagram of the test rig. The sliding test was performed at sliding speeds of 0.11–0.77 m s⁻¹ and loads of 2.0–10.0 N under dry,

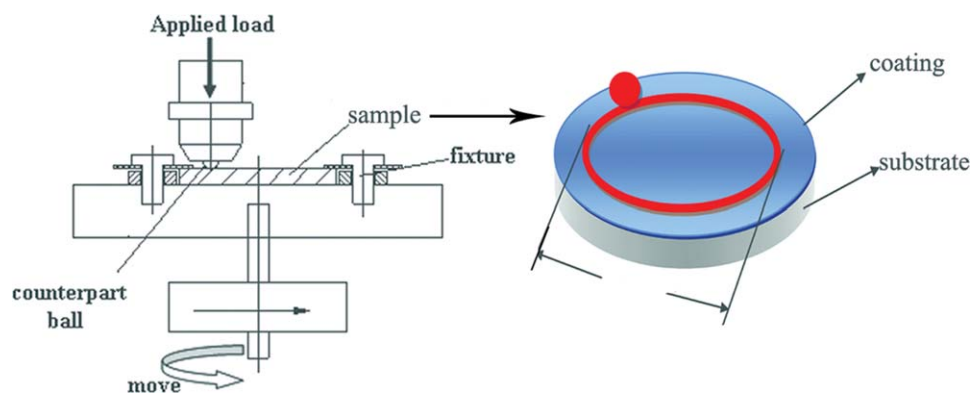


Figure 1. Schematic diagram of the wear test for the coatings. [Color figure can be viewed in the online issue, which is available at wileyonlinelibrary.com.]

mechanical oil or water sliding condition for 60 min. After wear test, line profile of wear track was measured using a surface profile measurement system (BMT Expert 3D, Germany). Width and depth of wear track were converted into wear volume by the equipment software automatically. The wear rates of all the coatings were calculated from $K = V/S \cdot F$, where V is the wear volume (mm^3), S the total sliding distance (m) and F the normal load (N). Three replicate friction and wear tests were carried out for each specimen and the average of three replicate results was reported together with their errors. After sliding, worn surfaces of the coatings and their corresponding counterpart balls were analyzed using the Quanta 200 SEM.

RESULTS AND DISCUSSION

FTIR Spectra of the Pure and Modified Nano-Si₃N₄

Figure 2 shows FTIR spectra of the pure and treated nano-Si₃N₄. The peak at 3500 cm^{-1} in the pure nano-Si₃N₄ was ascribed to stretching band of hydroxyl group. This peak disappeared in the treated nano-Si₃N₄. Some new peaks were observed in the treated nano-Si₃N₄ compared to the untreated

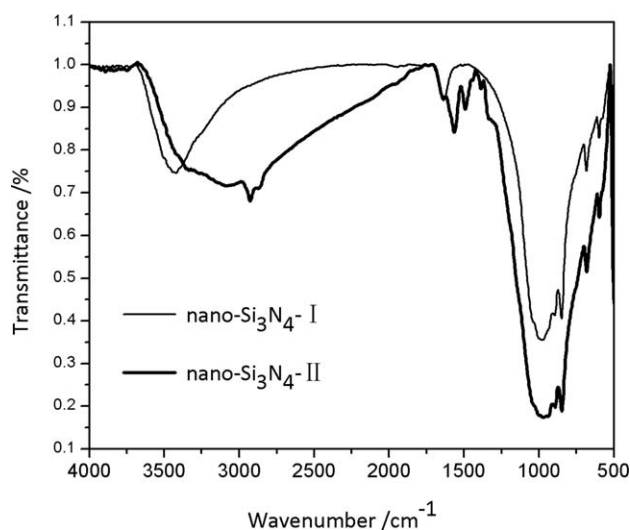
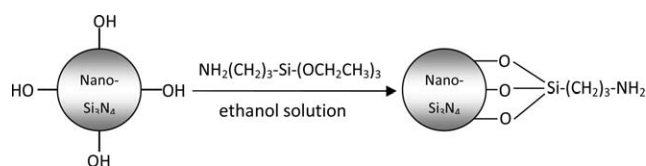


Figure 2. FTIR spectra of pure (nano-Si₃N₄-I) and treated nano-Si₃N₄ (nano-Si₃N₄-II).

one. The peaks at 2850 and 2925 cm^{-1} in the treated nano-Si₃N₄ belonged to characteristic stretching bands from methylene and methyl group. The bands at 1000 – 1100 cm^{-1} resulting from the contributions from Si—O—Si stretching bands were broadened in the treated nano-Si₃N₄. The peak at 3300 cm^{-1} in the treated nano-Si₃N₄ was assigned to stretching vibration of N—H. The results showed that nano-Si₃N₄ was successfully grafted with KH-550 by the modification process. The possible chemical reaction might be as follows:



Friction and Wear Performances

Table I compares the friction coefficients and wear rates of different coatings at 4.0 N , 0.33 m s^{-1} and dry sliding condition. Incorporation of 20 wt % PTFE greatly reduced the friction coefficient and wear rate of the PI coating, which might be attributed to self-lubricative PTFE that reduced the friction and shear force caused by the applied load. The addition of nano-Si₃N₄ further improved the friction reduction and wear resistance of PI/PTFE composite coating. The treated nano-Si₃N₄ is much better than the untreated one, as shown in Table I. Coating-IV exhibited the lowest wear rate and friction coefficient. Its wear rate was more than one order of magnitude lower and its friction coefficient was over two times smaller than that of Coating-I. The reinforcing mechanism of the modified nano-Si₃N₄ will be illustrated in the later sections.

Typical friction coefficient curves of different coatings with increasing sliding distance at 4.0 N , 0.33 m s^{-1} and dry sliding condition are shown in Figure 3. The friction coefficient of pure PI coating was much higher than those of other composite coatings in whole sliding process. Surprisingly, no great differences were found concerning the variation of friction coefficient for these composite coatings. Meanwhile, it was observed that the friction coefficient of pure PI coating rapidly rose and reached over 0.30 after a short running distance $< 10 \text{ m}$.

Table I. Comparisons of the Friction Coefficients and Wear Rates of the Different Coatings at 4.0 N, 0.33 m s⁻¹ and Dry Sliding Condition

Samples	Compositions	Friction and wear performance	
		Friction coefficient (μ)	Wear rate/ 10 ⁻⁴ mm ³ (N m ⁻¹) ⁻¹
Coating-I	Pure PI	0.346	2.736
Coating-II	PI/20 wt %PTFE	0.149	1.313
Coating-III	PI/20 wt %PTFE/5 wt %nano-Si ₃ N ₄ -I	0.145	0.545
Coating-IV	PI/20 wt %PTFE/5 wt %nano-Si ₃ N ₄ -II	0.140	0.244

However, the composite coatings experienced a long steady increase up till reaching 0.15 at 400 m of sliding distance and then maintained this level till the end of the test, which might be due to the incorporations of self-lubricative PTFE and nano-Si₃N₄ particles.

Figure 4 compares the friction coefficient and wear rate of the PI/PTFE composite coating doped with 5 wt % untreated and

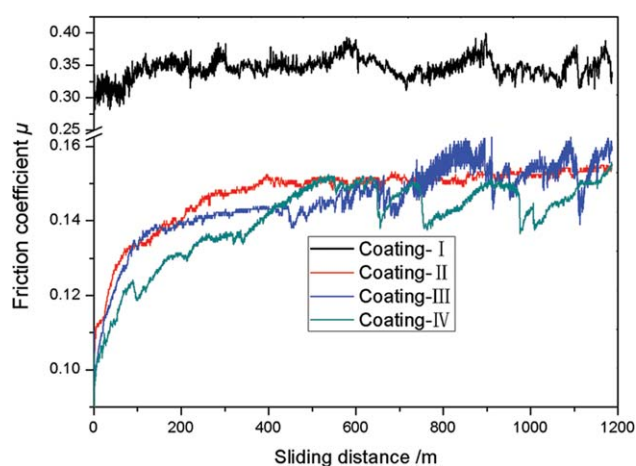
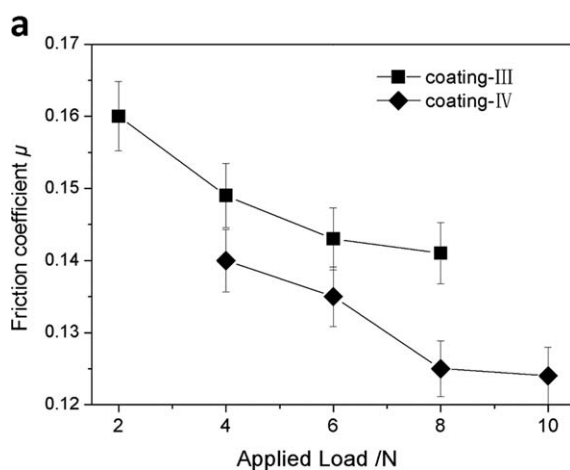


Figure 3. Typical friction coefficient curves of various composite coatings with increasing sliding distance at 4.0 N, 0.33 m s⁻¹ and dry sliding condition. [Color figure can be viewed in the online issue, which is available at wileyonlinelibrary.com.]



treated nano-Si₃N₄ with increasing applied loads at 0.33 m s⁻¹ and dry sliding condition. The nanocomposite coating filled with the modified nano-Si₃N₄ displayed lower friction coefficient and better wear resistance than the coating filled with unmodified one, irrespective of the applied loads. Meanwhile, the friction coefficient of the nanocomposite coating decreased with increasing applied load [Figure 4(a)], which might be attributed to the decrease of real contact area between coating and steel ball with increasing applied load.² As shown in Figure 4(b), their wear rates increased with the increase of applied loads. The increasing applied load always induces more severe plastic deformation for the composite coatings owing to increasing mechanical incompatibility between the soft coating and the hard steel substrate.²⁴ Severe plastic deformation caused serious adhesion and fatigue wear and then increased the wear rate of the coating with increasing applied loads.

Effect of modified nano-Si₃N₄ content on the friction coefficients and wear rates of the composite coating at 0.33 m s⁻¹, 4.0 or 6.0 N and dry sliding condition are shown in Figure 5. The composite coating had low friction coefficient between 0.130 and 0.145. Generally, the friction coefficients of the nanocomposite coatings decreased with the increase of the modified nano-Si₃N₄ content. Moreover, the friction coefficients of the coatings at 6.0 N were slightly lower than those at 4.0 N, which was independent of the content of nano-Si₃N₄. However, the wear rate decreased with increasing nano-Si₃N₄ content up to 5 wt %, and then increased with the further increase of the nano-

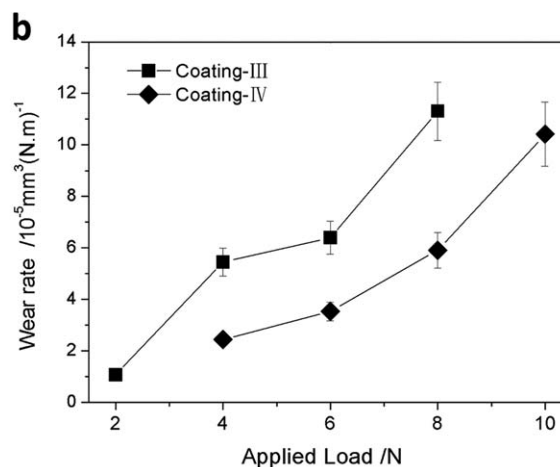


Figure 4. Variations of friction coefficient (a) and wear rate (b) of the composite coatings filled with 5 wt % untreated and treated nano-Si₃N₄ with increasing applied load at 0.33 m s⁻¹ and dry sliding condition.

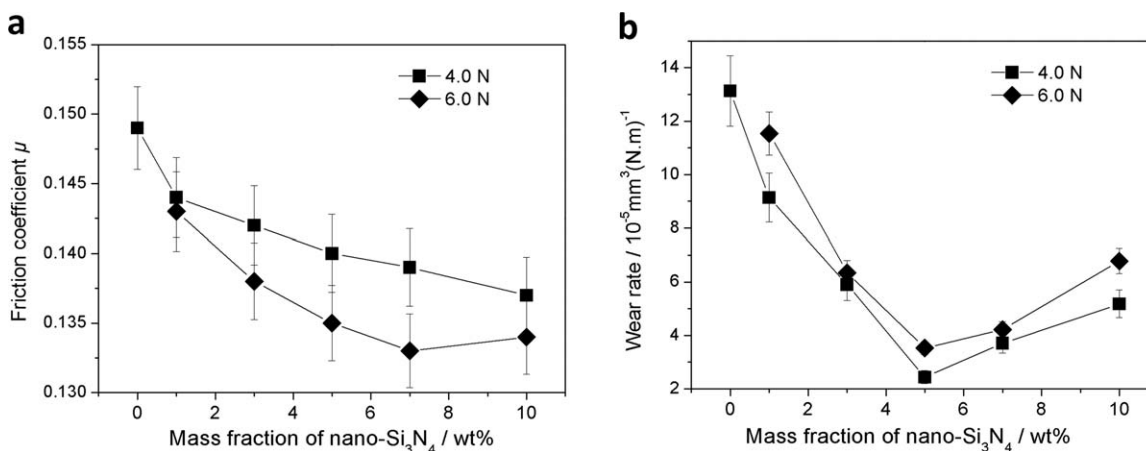


Figure 5. Effect of the modified nano-Si₃N₄ content on the friction coefficient (a) and wear rate (b) of the nanocomposite coating at 0.33 m s⁻¹, 4.0 or 6.0 N and dry sliding condition.

Si₃N₄ content. The wear rate of the coating filled with 5 wt % modified nano-Si₃N₄ was more than five times smaller than that of the unfilled one. It was concluded that the optimal content of the modified nano-Si₃N₄ in the nanocomposite coating was 5 wt %. Figure 5 also exhibits that the wear rates of the nanocomposite coatings at 6.0 N are slightly higher than those at 4.0 N.

Figure 6 displays the variations of the friction coefficient and wear rate of Coating-IV with increasing sliding speed at 8.0 N and dry sliding condition. The friction coefficient increased with increasing sliding speed. With the increase of the sliding speed, the contact area between coating and steel ball increase, which results in the increase of friction force because it is proportional to the actual contact area. Interestingly, the wear rate decreased with increasing sliding speed up to 0.55 m s⁻¹ and then increased with the further increase of sliding speed. An important factor that affects wear rate is sliding distance, *S*, because the coefficient value is negative. The wear rate always decreases with increasing speed for range of parameters tested. It could be concluded that the decreasing wear rate for this

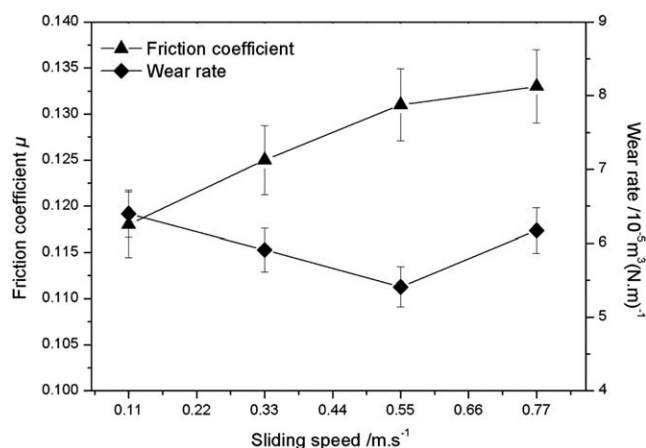


Figure 6. Variations of friction coefficient and wear rate of Coating-IV with increasing sliding speed at 8.0 N and dry sliding condition.

nanocomposite coating with the increase of sliding speed up to 0.55 m s⁻¹ derived from the rapid increase of sliding distance. However, the wear rate rapidly increased as the sliding speed increased to 0.77 m s⁻¹, which might be attributed to the rapid increase of friction-induced heat at extreme high sliding speed.^{1,2} The increase of the friction-induced heat prompts the plastic deformation of the matrix resin and then induces the catastrophic failure of the coating during sliding process.

To broaden the applications of this nanocomposite coating as engineering materials under various sliding environments, Table II compares the friction coefficients and wear rates of Coating-IV under dry, water and mechanical oil sliding environment. The coating exhibited the lowest friction coefficient under oil sliding condition, followed by under the water sliding condition. However, the wear rates of the coating were very high when it slid steel under water or oil environment, which suggested that the composite coating was unsuitable to apply in water or oil sliding condition. The composite coating displayed the highest wear rate under water sliding environment among all test conditions. The sharp decrease of the wear resistance at water or oil resulted from the corrosion wear occurred at these sliding conditions, which was confirmed by the SEM analysis of the worn surfaces in the followed section.

SEM and FTIR Analysis

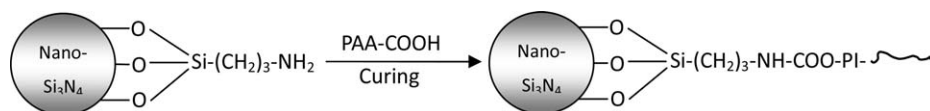
Typical SEM images of the cross-section and the surface of Coating-IV and its element distribution are shown in Figure 7. As shown in Figure 7(a), the nanocomposite coating bonded well with the steel substrate due to blurry interface between the coating and the substrate. Moreover, no gaps or cavities were observed at the cross-section of the coating, as indicated by Figure 7(a). As shown in Figure 7(b), most of PTFE particles that appeared white against the gray PI matrix had a uniform dispersion in the matrix. The disperse size of PTFE particle in the coating were around 5.0 μm . As shown in Figure 7(d,e), it was clear that the elements of F and Si uniformly dispersed on the surface of Coating-IV, which indicated the good dispersions of PTFE and modified nano-Si₃N₄ particles in the nanocomposite coating.

Table II. Comparisons of the Friction Coefficients and Wear Rates of Coating-IV Under Different Sliding Environment at 0.33 m s⁻¹, 6.0, and 8.0 N

Test condition and properties	Friction coefficient (μ)		Wear rate/ 10^{-5} mm ³ (N m) ⁻¹	
	6.0 N	8.0 N	6.0 N	8.0 N
Dry sliding condition	0.135	0.125	3.53	5.91
Water sliding condition	0.120	0.104	38.5	62.7
Oil sliding condition	0.052	0.044	16.2	23.9

Because of small size effect, nanoparticle is easy to agglomerate if no specific surface treatment was applied beforehand. In this work, nano-Si₃N₄ was modified by grafting the silane coupling agent of KH550 (Figure 2). The filler/matrix adhesion might be substantially enhanced by chain entanglement and/or chemical

groups at 1153 cm⁻¹ were revealed in Coating-IV. These results indicated the amino from KH550 grafted onto the surface nano-Si₃N₄ might react with the carboxyl in the PAA-COOH resin during the curing process. The chemical reaction might be as follows²⁷:



bonding between the chemical function groups grafted on the nanoparticles and the adhesive resin during the curing process of the composite coating. Figure 8 displays FTIR spectra of pure PAA-COOH and Coating-IV. The broad band near 3400 cm⁻¹ and the peak at 1720 cm⁻¹ shown in PAA-COOH resin are characteristic peaks of carboxyl. The peak at 1720 cm⁻¹ disappeared and the band near 3400 cm⁻¹ was broadened in Coating-IV, which might derive from produced amide groups. Moreover, the peaks of Si-O-Si bond at 1073 cm⁻¹ and Si-O

Accordingly, it is rational that the nanocomposite coating filled with the modified nano-Si₃N₄ had better tribological properties than the coating filled with the untreated one, as shown in Table I and Figure 4.

SEM images of the worn surfaces of the different coatings after sliding at 4.0 N and 0.33 m s⁻¹ are shown in Figure 9. As shown in Figure 9(a), the worn surface of the pure PI coating (Coating-I) displayed obvious signs of cracks, scuffing and

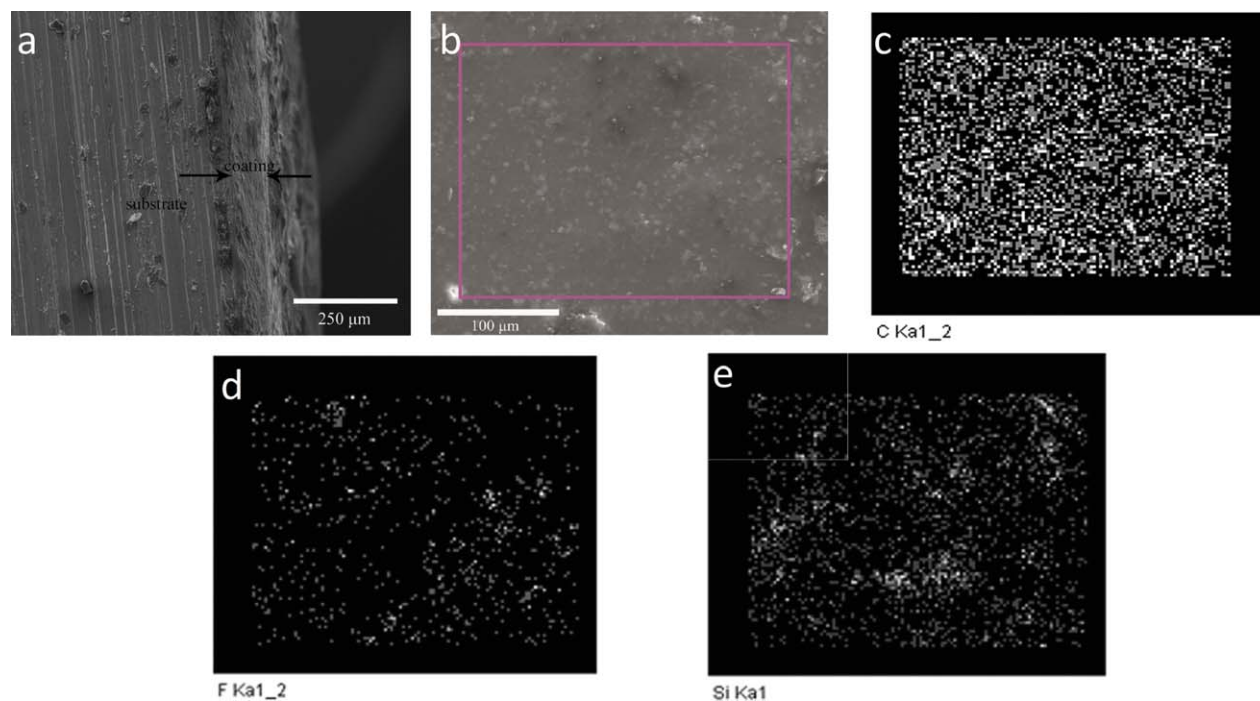


Figure 7. Typical SEM images of the cross-section and surface of Coating-IV and its element distribution (a: cross-section; b: Surface; c: C element distribution on (b); d: F element distribution on (b); e: Si element distribution on (b)). [Color figure can be viewed in the online issue, which is available at wileyonlinelibrary.com.]

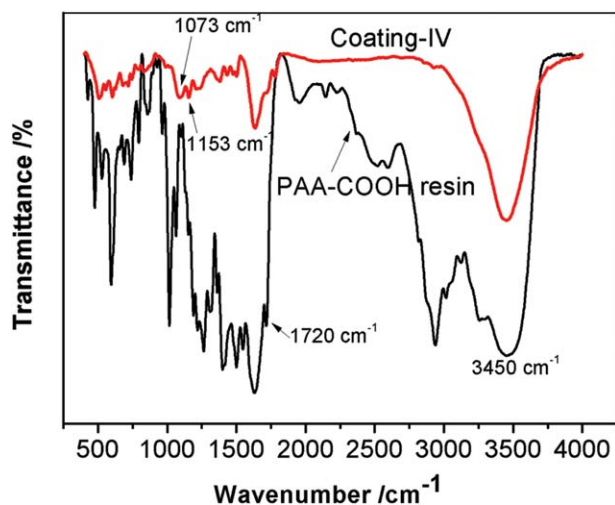


Figure 8. FTIR spectra of the adhesive resin of PAA-COOH and Coating-IV. [Color figure can be viewed in the online issue, which is available at wileyonlinelibrary.com.]

serious plastic deformation. The results suggested the severe adhesion and fatigue wear occurred for the pure PI coating. The worn surface of Coating-II did not have crack but also displayed plastic deformation and scuffing, as shown in Figure 9(b). In the case of Coating-III, the worn surface was smoother than that of Coating-I and Coating-II, as shown in Figure 9(c). But signs of cracks and adhesion were found on this worn surface. Unsurprisingly, the worn surface of Coating-IV [Figure 9(d)] was very smooth and had few cracks and slight scuffing, which accorded well with its best wear resistance and friction reduction. The wear mechanism of Coating-IV was slight fatigue and adhesive wear.

Figure 10 compares the worn surfaces of the composite coatings incorporated with different content of the modified nano-Si₃N₄ at various sliding conditions. The worn surface of the composite coating filled with 1 wt % nano-Si₃N₄ at 6.0 N and 0.33 m s⁻¹ was very rough and showed severe plastic deformation and scuffing [Figure 10(a)]. As the modified nano-Si₃N₄ content increased to 5 wt %, the coating displayed smooth worn surface

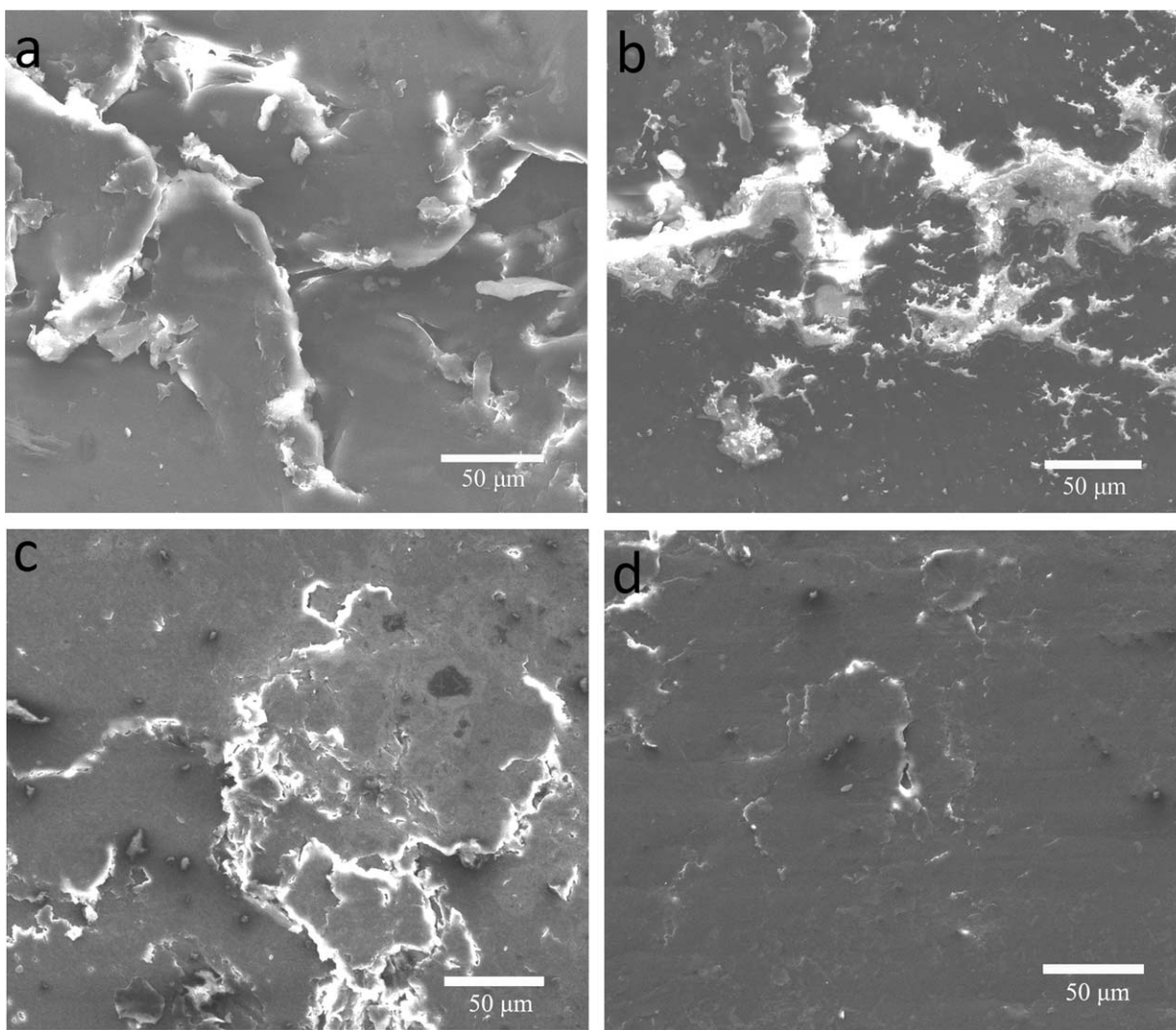


Figure 9. SEM images of the worn surfaces for different coatings after sliding at 4.0 N and 0.33 m s⁻¹ (a: Coating-I; b: Coating-II; c: Coating-III; d: Coating-IV).

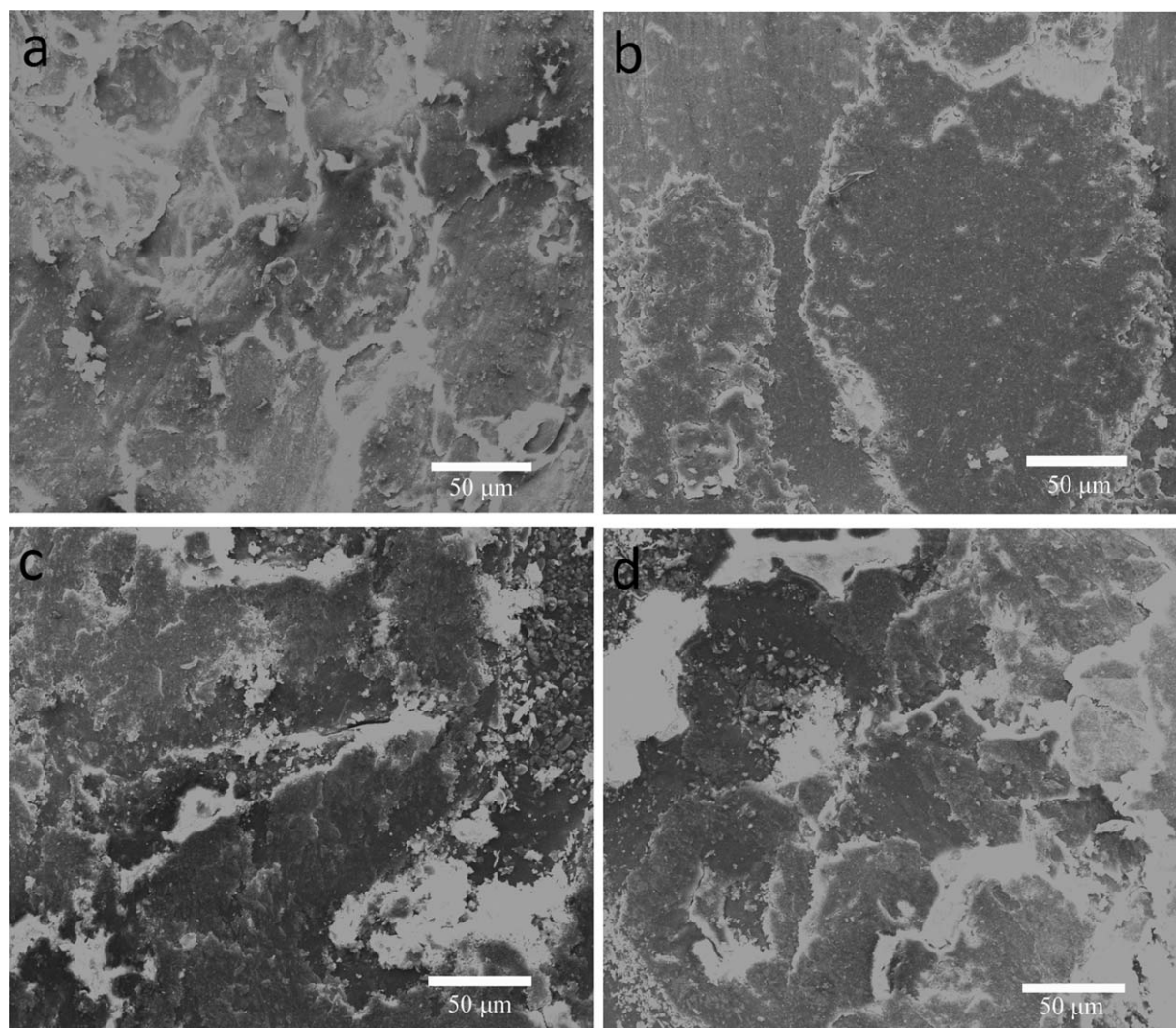


Figure 10. SEM pictures of the worn surfaces of PI/PTFE composite coatings with different content of modified nano-Si₃N₄ at various sliding conditions (a: 1 wt % nano-Si₃N₄, 6.0 N and 0.33 m s⁻¹; b: 5 wt % nano-Si₃N₄, 6.0 N and 0.33 m s⁻¹; c: 10 wt % nano-Si₃N₄, 6.0 N and 0.33 m s⁻¹; d: 5 wt % nano-Si₃N₄, 8.0 N and 0.77 m s⁻¹).

that was featured with slight scratches and adhesive wear [Figure 10(b)], which corresponded to the decreased wear rate with increasing nano-Si₃N₄ up to 5 wt % (Figure 5). However, the worn surface of the composite coating incorporated with 10 wt % nano-Si₃N₄ was very rough and characterized with the cracks, severe scuffing and plastic deformation, as shown in Figure 10(c). In addition, it seemed that many nano-Si₃N₄ particles were enriched at certain locations of the worn surface. The incorporation of excessive nanoparticles induced the non uniform dispersion of the particles in matrix and then affected the structure integrity of the coating.³ Accordingly, the nanocomposite coating was easily scuffed and abraded by counterpart steel ball during the sliding process. As shown in Figure 10(d), the worn surface of the coating was featured with severe scuffing and even peeling-off as it slid the counterpart ball at 8.0 N and 0.77 m s⁻¹. The higher friction-induced heat caused by the high sliding speed and applied load resulted in relaxation of PI molecular chain and prompted plastic deformation of the

matrix resin, which finally induced catastrophic failure of the coating during this sliding process.^{7,28}

Figure 11 presents SEM micrographs of the transfer films formed on the counterpart steel balls sliding against various coatings under 4.0 N and 0.33 m s⁻¹. As shown in Figure 11(a), the transfer film formed on the counterpart ball sliding against Coating-I was very thick, lumpy and discontinuous, which corresponded to the severe adhesive wear for pure PI coating. Serious scuffing and deep ploughs were observed on the worn surface of this counterpart ball. The worn surface of the counterpart ball sliding against Coating-II became smooth, and plucked scars and deep ploughs were not found on this surface. Nevertheless, the transfer film formed on this ball was also thick and discontinuous [Figure 11(b)]. Interestingly, the worn surface of the counterpart ball sliding against Coating-III was thin and uniform but showed a few signs of scuffing, as shown in Figure 11(c), which agreed well with the better wear

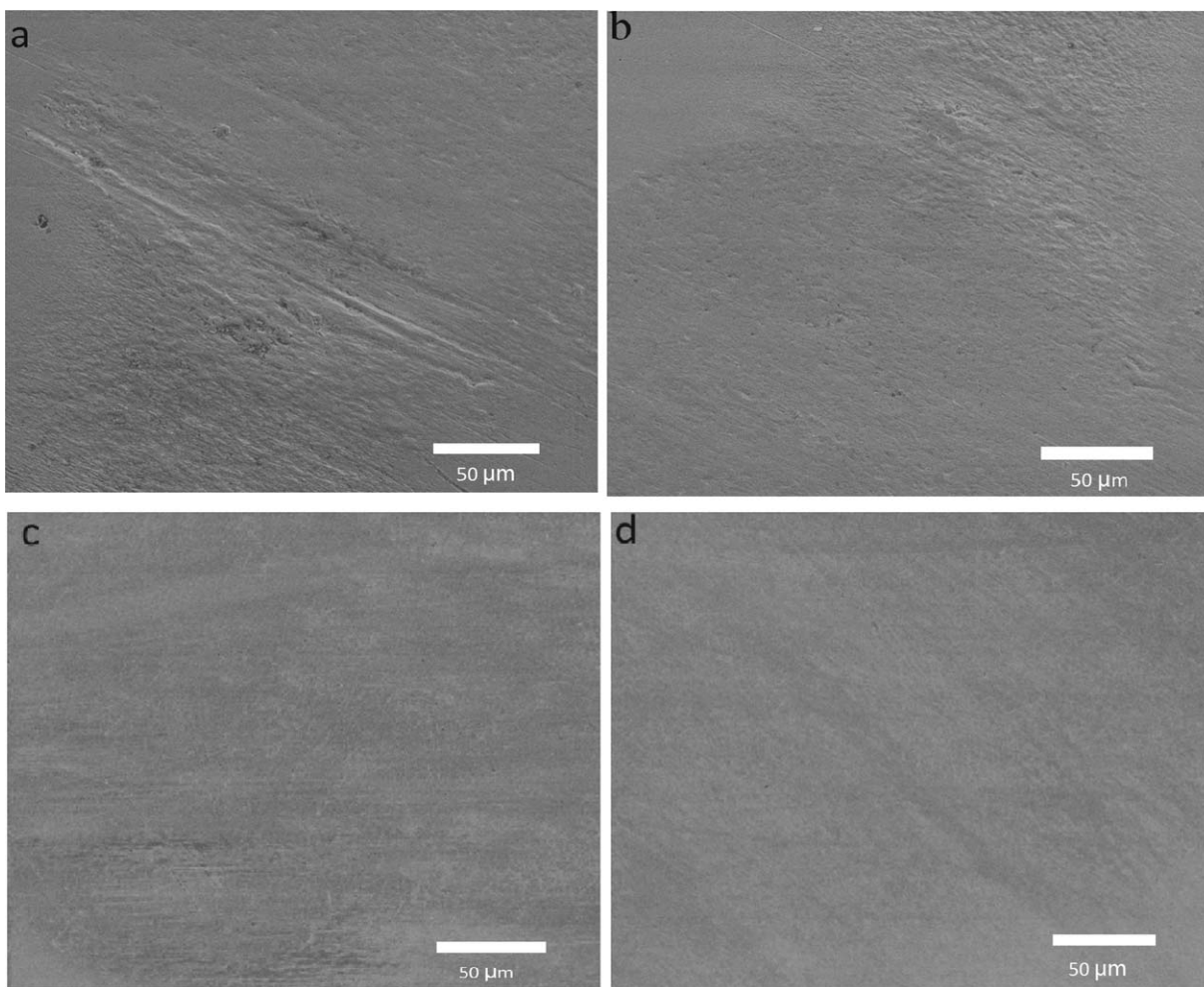


Figure 11. SEM micrographs of the counterpart steel ball sliding against different coatings under 4.0 N and 0.33 m s^{-1} (a: Coating-I; b: Coating-II; c: Coating-III; d: Coating-IV).

resistance and friction reduction of Coating-III compared to Coating-I and Coating-II (Table I). As shown in Figure 11(d), the worn surface the counterpart ball sliding against Coating-IV was very smooth. The transfer film formed was very thin, uniform and coherent, which was related to the best friction and wear performance of this coating. The characteristic of transfer films formed on the counterpart balls sliding accounted for the friction and wear behaviors of these coatings.

The worn surfaces of Coating-IV and its corresponding counterpart balls at 6.0 N, 0.33 m s^{-1} and different sliding environment are shown in Figure 12. The worn surface under water sliding condition was featured with typical corrosive patches, scuffed grooves and cracks, as shown in Figure 12(a). It was seemed that nanoparticles were enriched on the worn surface, which might result from that the matrix resin in wear debris was washed away by water during sliding process. The enriched nanoparticles in worn surface induced relatively high friction coefficient for the coating under water sliding condition (Table II). As shown in Figure 12(b), the worn surface of the coating became smooth but also displayed obvious corrosion wear under oil sliding condition. The corrosiveness of water and oil led to poor wear resistance for the coat-

ing under these conditions. The counterpart balls sliding against Coating-IV under water and oil sliding condition displayed scratches and fine grooves, as shown in Figure 12(c,d). In addition, no signs of the transfer film were observed on the two counterpart balls, which also had relation with the high wear rate of Coating-IV under oil and water sliding environment.

CONCLUSIONS

The incorporation of PTFE particles improved the friction reduction and wear resistance of PI coating. The addition of nano- Si_3N_4 nanoparticles further decreased the friction coefficient and wear rate of the composite coating. The friction and wear performances of the composite coating were greatly affected by the modification and the mass fraction of nano- Si_3N_4 in the coating. The modified nano- Si_3N_4 was much better than the untreated one. The PI based coating incorporated with 20 wt % PTFE and 5 wt % modified nano- Si_3N_4 displayed the best wear resistance and friction reduction.

Sliding conditions, including applied loads, sliding speeds, and sliding environments greatly affected the friction and wear

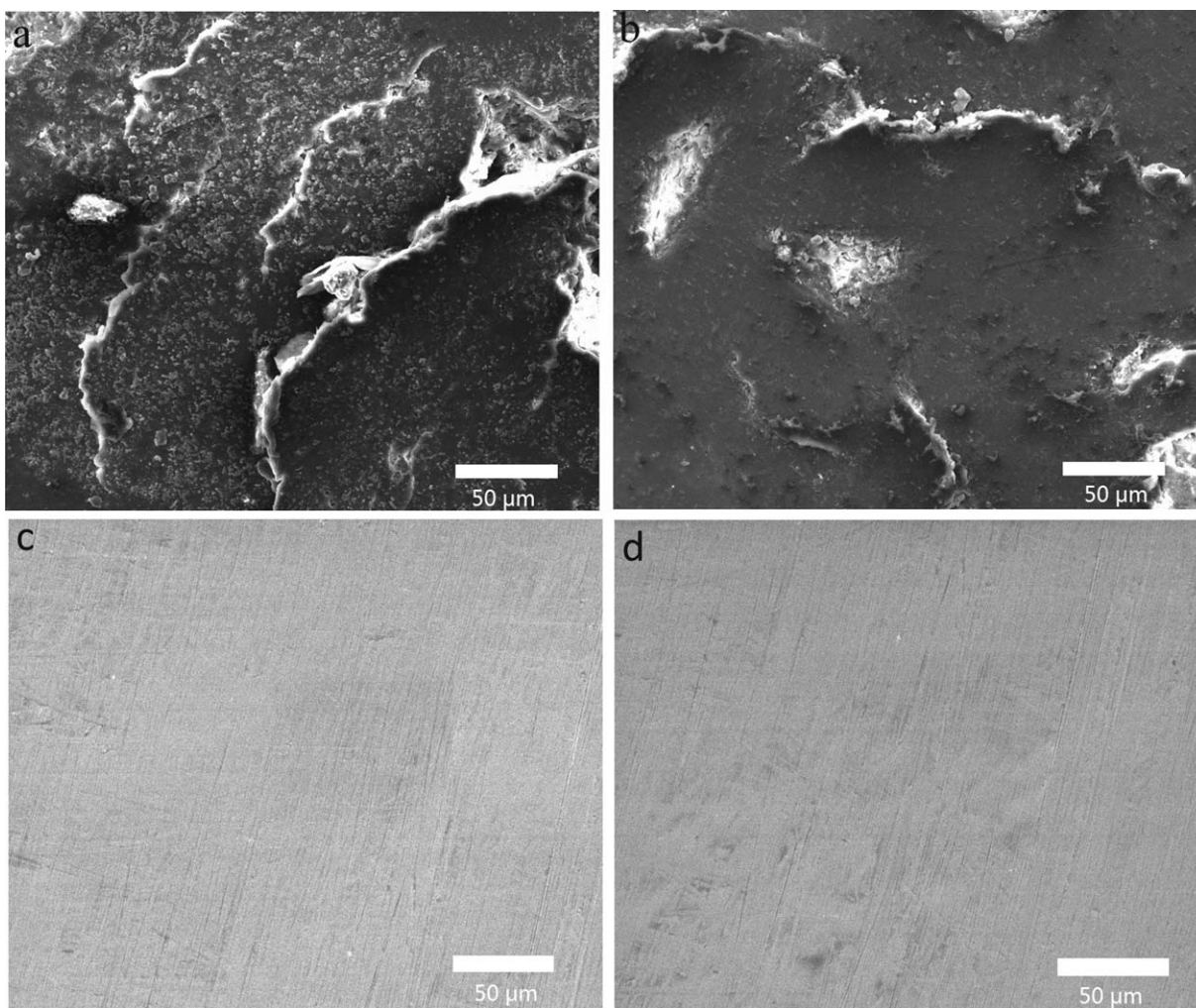


Figure 12. SEM pictures of the worn surfaces for Coating-IV and its corresponding counterpart ball after sliding at 6.0 N, 0.33 m s^{-1} , and different sliding environments (a and c: under water condition; b and d: under oil condition).

performances of the nanocomposite coatings. The coating was unsuitable to apply under water or oil sliding environments due to corrosiveness of water and oil to the coating. Differences in the friction and wear behavior of the coating as the function of the filler or sliding condition were attributed to the nature and dispersion of the filler, the characteristic of transfer film formed on the counterpart ball, and the wear mechanism of the coating under different sliding conditions.

ACKNOWLEDGMENTS

The authors are grateful to the financial support of the National Natural Science Foundation of China (Grants: 51275176), Pearl River Science and Technology Star (2012J2200068) and Fundamental Research Funds for the Central Universities (Grant: 2014 ZG0014).

REFERENCES

1. Song, H. J.; Zhang, Z. Z. *Tribol. Int.* **2008**, *41*, 396.
2. Song, H. J.; Zhang, Z. Z. *Surf. Coat. Tech.* **2006**, *201*, 1037.
3. Kang, Y.; Chen, X.; Song, S.; Yu, L.; Zhang, P. *Appl. Surf. Sci.* **2012**, *258*, 6384.
4. Zhang, H.; Tang, L.; Zhang, Z.; Gu, L.; Xu, Y.; Eger, C. *Tribol. Int.* **2010**, *43*, 83.
5. Men, X. H.; Zhang, Z. Z.; Song, H. J.; Wang, K.; Jiang, W. *Compos. Sci. Technol.* **2008**, *68*, 1042.
6. Fusaro, R. L. *ASLE. Trans.* **1978**, *21*, 125.
7. Cai, H.; Yan, F.; Xue, Q. *Mater. Sci. Eng. A* **2004**, *364*, 94.
8. Zhang, X. R.; Pei, X. Q.; Wang, Q. H. *Mater. Des.* **2009**, *30*, 4414.
9. Shi, Y.; Mu, L.; Feng, X.; Lu, X. *Mater. Des.* **2011**, *32*, 964.
10. Li, J.; Cheng, X. H. *J. Appl. Polym. Sci.* **2008**, *107*, 1737.
11. Shi, Y. J.; Mu, L. W.; Feng, X.; Lu, X. H. *J. Appl. Polym. Sci.* **2011**, *121*, 1574.
12. Pozdnyakov, A. O.; Kudryavtsev, V. V.; Friedrich, K. *Wear* **2003**, *254*, 501.
13. Kim, J.; Im, H.; Cho, M. H. *Wear* **2011**, *271*, 1029.

14. Balaji, V.; Tiwari, A. N.; Goyal, R. K. *Polym. Eng. Sci.* **2011**, *51*, 509.
15. Unal, H.; Mimaroglu, A. *Wear* **2012**, *271*, 132.
16. Wang, Q.; Zhang, X.; Pei, X. *Mater. Des.* **2010**, *31*, 3761.
17. Zouari, M.; Kharrat, M.; Dammak, M. *Surf. Coat. Tech.* **2010**, *204*, 2593.
18. Kumar, M.; Satapathy, B. K.; Patnaik, A.; Kolluri, D. K.; Tomar, B. S. *J. Appl. Polym. Sci.* **2012**, *124*, 3650.
19. Li, D.-X.; Li, W.-J.; Xie, Y.; Li, X.-X. *J. Appl. Polym. Sci.* **2012**, *124*, 4239.
20. Su, F. H.; Zhang, Z. Z.; Liu, W. M. *Wear* **2008**, *265*, 311.
21. Sawyer, W. G.; Freudenberg, K. D.; Bhimaraj, P.; Schadler, L. S. *Wear* **2008**, *254*, 573.
22. Blanchet, T. A.; Kandanur, S. S.; Schadler, L. S. *Tribol. Lett.* **2010**, *40*, 11.
23. Friedrich, K.; Zhang, Z.; Schlarb, A. K. *Compos. Sci. Technol.* **2005**, *65*, 2329.
24. Song, H. J.; Zhang, Z. Z.; Men, X. H. *Surf. Coat. Tech.* **2006**, *201*, 3767.
25. Zhang, H. J.; Zhang, Z. Z.; Guo, F.; Liu, W. M. *Polym. Eng. Sci.* **2009**, *49*, 115.
26. Zhang, X.; Pei, X.; Zhang, J.; Wang, Q. *Colloid. Surf. A* **2009**, *339*, 7.
27. He, S.; Lu, C.; Zhang, S. *ACS Appl. Mater. Inter.* **2011**, *3*, 4744.
28. Zhang, X.; Pei, X.; Wang, Q. *J. Appl. Polym. Sci.* **2009**, *111*, 2980.